Tailoring phonon band structures with broken symmetry by shaping spatiotemporal modulations of stiffness in a one-dimensional elastic waveguide

Pierre A. Deymier,[1] Vitthal Gole,[1] Pierre Lucas,[1] Jérôme O. Vasseur,[2] and Keith Runge[1]
[1]*Department of Materials Science and Engineering, University of Arizona, Tucson, Arizona 85721, USA*
[2]*Institut d'Electronique, de Micro-électronique et de Nanotechnologie, UMR CNRS 8520, Cité Scientifique, 59652 Villeneuve d'Ascq Cedex, France*
(Received 22 February 2017; revised manuscript received 6 July 2017; published 17 August 2017)

Spatiotemporal modulations of the elastic properties of materials can be used to break time and parity symmetry of elastic waves. We show that the form of the elastic band structure depends not only on the spatial and temporal periodicity of a spatiotemporal modulation but also on its shape through its Fourier components. We demonstrate that hybridization gaps open from interactions between the Bloch modes of the periodic medium in absence of the temporal variation of the modulation and the combined sinusoidal components of the Fourier decomposition of the periodic modulation.

DOI: 10.1103/PhysRevB.96.064304

I. INTRODUCTION

Several approaches offer pathways to access the deliberate design of elastic media with broken symmetry (inversion, time reversal, parity, chiral, particle-hole); symmetry can be broken either intrinsically or extrinsically. Symmetry breaking then may lead to nonreciprocity in wave propagation [1]. Symmetry in intrinsic systems is broken by different "internal" degrees of freedom such as through internal resonance [2] or symmetry-breaking structural features (e.g., inversion or chirality symmetry) [3–5] and without addition of energy from the outside. In contrast, energy can be added extrinsically to break symmetry. In this case, symmetry of elastic waves can be broken by moving fluids [6,7], gyroscopic inclusions [8], or directed and externally driven spatiotemporal modulations of the elastic properties of the medium [9–13]. For the sake of completeness, one may note that investigation of nonreciprocity in the propagation of electromagnetic waves [14–19] has preceded their elastic counterparts.

Previous studies [9–13] have theoretically and computationally demonstrated that time-reversal symmetry can be broken by creating a moving-superlattice-like spatial modulation of the elastic constants in a one-dimensional elastic medium. The symmetry breaking, in a time-dependent superlattice leads to bulk phonon modes with nonconventional topology, which do not possess the conventional mirror symmetry in momentum space [9–13]. In all cases, the spatiotemporal modulation results in effects such as frequency splitting of a monochromatic incident signal that is analogous to Brillouin scattering [10]. In previous work, such as Ref. [9], sinusoidal modulations were typically used. Here we study how the shape of the periodic spatially varying modulation of a material's elastic constants affects the nonreciprocal band structure. Using a one-dimensional model of an elastic medium, we consider three different shapes of the spatiotemporal modulation. These modulations, each traveling at the same velocity, are one-dimensional superlattices with identical period in space but different shapes. The three modulations include a periodic set of Gaussian functions and two Fourier expansions (in terms of sinusoidal functions) of the Gaussian modulation at different orders of truncation. The lowest order expansion corresponds to a single sinusoidal modulation, and the higher order expansion includes multiple sinusoidal terms that will be shown to simultaneously interact with elastic waves to open additional asymmetric band gaps in the elastic band structure. We calculate the band structures associated with the three modulations using the spectral energy density (SED) method [20], and conduct a theoretical analysis, within the framework of multiple time scale perturbation theory, of the origin of the symmetry breaking and of formation of asymmetric band gaps. We demonstrate unambiguously in this paper that the shape of the periodic spatiotemporal modulation which determines the number and characteristics of the sinusoidal components in its Fourier series expansion leads to nonlinear effects that involve low order interactions between the elastic waves and the individual Fourier components, but also importantly higher order interactions between elastic waves and combinations of Fourier components. The principal result of the present study is therefore that interactions with multiple Fourier components of a generally shaped modulation offer another pathways and a rich parameter space to deliberately design elastic wave band structure with broken symmetry.

In Sec. II of this paper we present a one-dimensional model of an elastic medium subjected to three related spatiotemporal modulations of the material's stiffness. These modulations, each traveling at the same velocity, are one-dimensional superlattices with identical period in space but different shapes. The more general superlattice takes the form of a periodic set of Gaussian functions. The other two superlattices represent Fourier expansions (in terms of sinusoidal functions) of the general superlattice at different orders of truncation. The lowest order of truncation actually corresponds to a single sinusoidal modulation. The present study demonstrates clearly that the next order in truncation includes multiple sinusoidal terms that combine and simultaneously interact with elastic waves to open additional asymmetric band gaps in the elastic band structure. The results of SED calculations are reported in Sec. III. A theoretical analysis, within the framework of multiple time scale perturbation theory, of the origin of symmetry breaking and of the formation of asymmetric elastic band gaps due to the combined effect of multiple Fourier components of the modulation, is also reported in Sec. III. For the sake of tractability, we consider the interaction of elastic waves with a modulation composed

of only two superposed sinusoidal Fourier components. The two components have different spatial characteristics but are subjected to identical temporal evolutions. We demonstrate in this section that the nonlinear interactions between elastic waves and the two combined sinusoidal components indeed lead to a rich parameter space for the design and control of the conditions for breaking symmetry of elastic wave band structures. Conclusions and contextualization of this work are presented in Sec. IV. In particular, having demonstrated that the shape of a modulation extends the realm of parameters that can be used to tailor elastic band structures beyond the spatial and temporal periodicities, this work suggests the possibility of creating on-demand functions such as nonreciprocity than can be programmed into—and elicited from—a material's "microstructure" topography (shape of the modulation and therefore the components of its Fourier series) in addition to its time evolution.

II. MODEL AND METHODS

We consider the propagation of longitudinal elastic waves along a one-dimensional material supporting spatial and temporal modulations of its stiffness. The giant photoelastic effects in chalcogenide glasses [21] are exploited to practically achieve the desired stiffness modulations by, for instance, illuminating the material with light of spatially and temporally varying intensity. Illuminating $GeSe_4$ chalcogenide glasses with near band gap laser radiation of increasing power results in a reduction of the longitudinal elastic constant (C_{11}) by nearly 50%. Depending on the power of the laser irradiating the glass, C_{11} values for $GeSe_4$ can vary between 9.2 (full power) to 18.4 GPa (zero power) [21]. This photo softening is athermal and reversible making it ideal as a means to realize time-dependent modulations. We assume constant density for $GeSe_4$($4361\,kg/m^3$), therefore the minimum and maximum values of C_{11} coincide with sound velocities of 1452 and 2054 m/s, respectively. The vibrational properties of the time-dependent elastic superlattices are investigated numerically. We represent the chalcogenide glass by a discrete one-dimensional mass-spring system with a spatial modulation of the stiffness of the springs that propagates in time with the velocity $+V$ (see schematic illustration in Fig. 1).

Individual masses ($m = 4.361 \times 10^{-9}$ kg) are equally spaced by $a = 0.1$ mm. This mass corresponds to that of a continuous segment of length a. The masses are connected by springs in which the spring constant varies between $\beta_{\min} = 920$ and $\beta_{\max} = 1840$ kN/m. The range of values of spring constants is therefore $\Delta\beta = 920$ kN/m.

For the calculation of the elastic band structure of the superlattice, we use a one-dimensional discrete chain model that contains $N = 3200$ masses with Born–von Karman boundary conditions, where the system takes the form of a ring. We have chosen the value of 100 intermass spacings for the period of the stiffness modulation, such that the period $L = 100a$. The system contains $N_C = 32$ cells of 100 masses each. This system is simulated using the method of molecular dynamics (MD).

We consider three spatiotemporal modulations of the material's stiffness with different but related shapes, as is shown in Fig. 2. The first modulation, named Gaussian superlattice, shown in Fig. 2(a), is constructed from the sum of a periodic set of Gaussian functions, where the stiffness of spring n is constructed from the following relation:

$$\beta_n^{(1)} = \beta_{\max} - \Delta\beta \sum_{i=-T}^{i=+T} e^{\left(\frac{-(x_n - x_i')^2}{2\sigma^2}\right)}, \tag{1}$$

with $x_i' = (i - \frac{1}{2})L$, $x_n = (n - \frac{1}{2})a$, and $\sigma = 8a$. T serves as a cut-off parameter which is a large enough integer beyond which contributions to the variation in stiffness are negligible. The other two superlattices represent expansions of the general Gaussian superlattice as a series of sinusoidal functions at different orders of truncation. The lowest order of truncation, shown in Fig. 2(b), corresponds to a single sinusoidal modulation with the same period as that of the Gaussian modulation. It is formulated analytically as

$$\beta_n^{(2)} = 0.75\beta_{\max} - 0.5\Delta\beta \sin\left(\frac{2\pi}{L}x_n\right). \tag{2}$$

The next order in truncation, shown in Fig. 2(c), includes three sinusoidal terms:

$$\beta_n^{(3)} = 0.9\beta_{\max} - 0.35\Delta\beta\left[\sin\left(\frac{2\pi}{L}x_n\right) - \frac{3}{4}\cos\left(2\frac{2\pi}{L}x_n\right) - \frac{1}{2}\sin\left(3\frac{2\pi}{L}x_n\right)\right]. \tag{3}$$

The time dependence of the three modulations is achieved by replacing x_n by $x_n - Vt$ where t is the time.

The dynamical trajectories generated by the MD simulation are analyzed within the framework of the spectral energy density (SED) method [20] for generating the elastic band

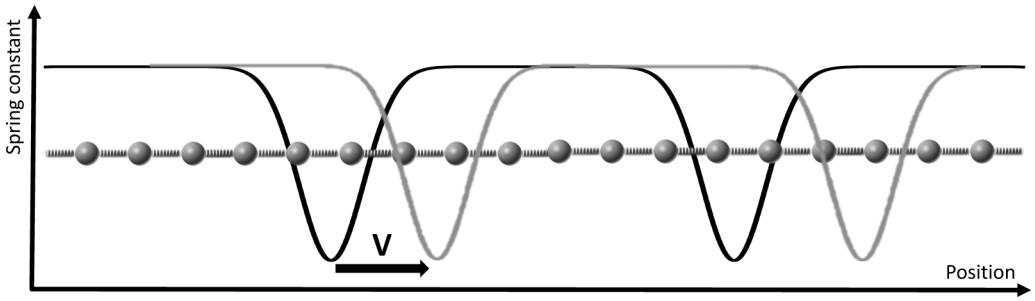

FIG. 1. Schematic representation of a one-dimensional mass spring system with periodically varying stiffness (spring constant) moving at a velocity V.

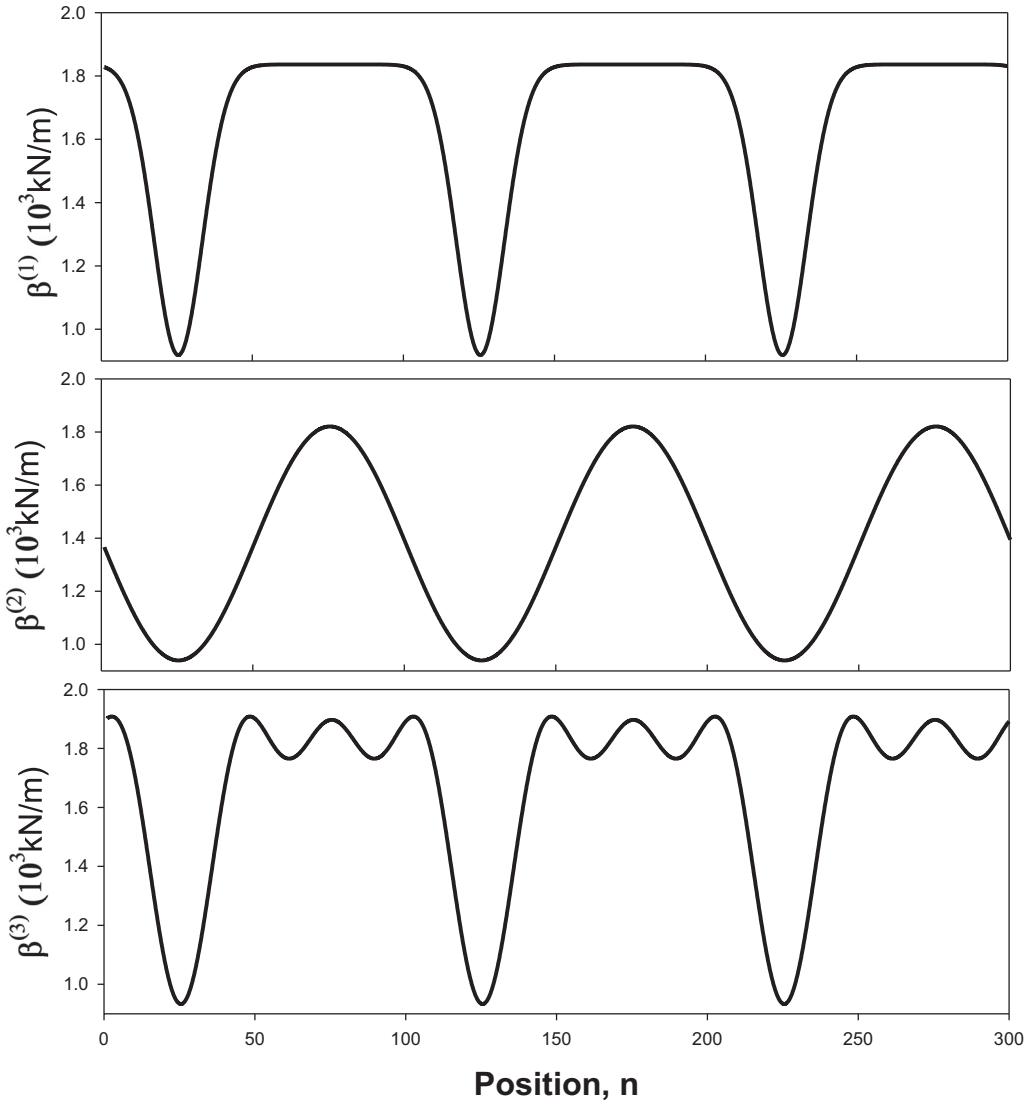

FIG. 2. Illustration of the three superlattices constructed by modulating the spring constant β_n over position n.

structure of the model superlattice. Formally, for a three-dimensional system, the expression for SED is written as follows:

$$\Phi(\vec{k},\omega) = \frac{1}{4\pi\tau_0 N}\sum_{\alpha}\sum_{b}^{B} m_b \times \left|\int_0^{T_0}\sum_{n_x}^{N} v_\alpha\left(\begin{matrix}n_x\\ b\end{matrix};t\right)e^{(i\vec{k}\cdot\vec{r_0}-i\omega t)}dt\right|^2,$$

where T_0 represents the length of time over which velocity data is collected, N is the total number of unit cells represented in the MD simulation, $v_\alpha(\begin{smallmatrix}n_{x,y,z}\\ b\end{smallmatrix};t)$ represents the velocity of mass m_b in unit cell $n_{x,y,z}$ in the α direction, and B is .... For a specified wave vector $(\vec{k})$, the spectrum relating SED to frequency is found by adding the square of the absolute value of the Fourier transform of the discrete temporal signal

$$f(t) = \sum_{n_{x,y,z}}^{N} v_\alpha\left(\begin{matrix}n_{x,y,z}\\ b\end{matrix};t\right)e^{(i\vec{k}\cdot\vec{r_0})}$$

for every $[\alpha, b]$ pair. The temporal Fourier transform is calculated using a fast Fourier transform algorithm. A SED value represents the average kinetic energy per unit cell as a function of wave vector and frequency. A peak in the spectrum relating SED to frequency signifies a vibrational eigenmode for wave vector $(\vec{k})$. In our one-dimensional system, the wave vector reduces to a wave number and we have 32 cells of 100 masses each. To ensure adequate sampling of the system's phase space, our reported SED calculations represent an average over four individual MD simulations each with time step $dt = 1.5$ ns and total simulation time of 2^{20} time steps.

III. RESULTS AND DISCUSSION

Figure 3 shows the calculated band structure of the Gaussian superlattice $\beta_n^{(1)}$ with velocities $V = 350$ m/s.

The time-dependent superlattice with spatial modulation $\beta_n^{(1)}$ and velocity $V = 350$ m/s possesses a band structure which exhibits a number of features in the form of faint additional bands and hybridization gaps. Note that the intensity

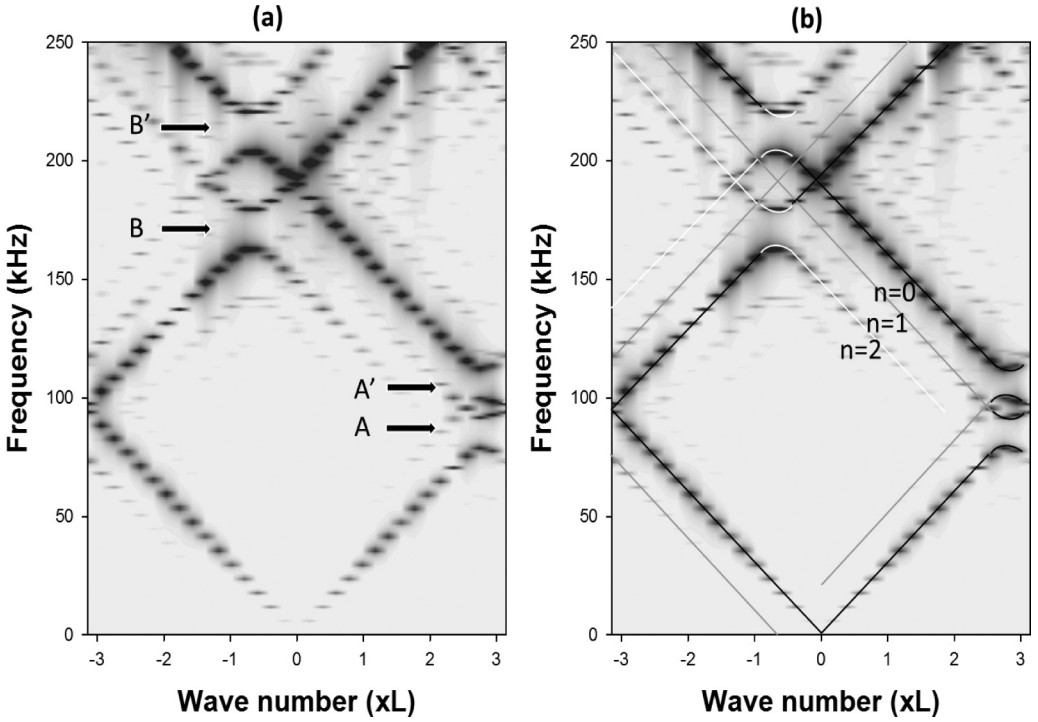

FIG. 3. (a) Band structures resulting from a moving periodic Gaussian modulations $\beta_n^{(1)}$. A and A' are band gaps arising from hybridization between zeroth-order modes $n = 0$ [static modulation and see Fig. 4(a)] and first-order modes ($n = 1$) resembling Stokes and anti-Stokes modes associated with Brillouin scattering due to the moving modulation. B and B' are hybridization gaps between second-order Stokes and anti-Stokes modes ($n = 2$) and zeroth-order modes. (b) Same band structure as (a) but with black, gray, and white solid lines serving as guides to the eyes and highlighting zeroth-order, first–order, and second-order modes, respectively. To enhance the contrast, the contour plots represent the SED intensity at the power 1/400. The frequency is in kHz and the wave number is in units of L.

of the bands relates to the sampling of the modes. The SED intensities are calculated as averages over four individual MD simulations. While this average is sufficient to observe all the modes relevant to this study, the relative intensity of the different modes may not be sampled efficiently.

We have shown previously that the interaction between elastic waves with frequency ν_0 and a spatiotemporal modulation of the elastic constants leads to a frequency splitting that resembles Brillouin scattering [10]. As will be demonstrated in the following theoretical analysis, the frequency of the Brillouin modes contains harmonics of the frequency associated with the moving modulation: $\upsilon_n = \upsilon_0 \pm nF$, where $F = \frac{\Omega}{2\pi} = \frac{V}{L}$ and $n = 1,2,3,\ldots$. These harmonic components appear as faint Stokes and anti-Stokes bands parallel to the folded bands of the static superlattice. The scattered modes hybridize with the static folded bands to form band gaps. The hybridization gaps form asymmetrically with respect to the wave number origin. For instance, the gaps A and A' in Fig. 3(a) result from the hybridization between a first-order Brillouin harmonic ($n = 1$) and the first and second zeroth-order bands of a static superlattice. These gaps occur in the positive wave number side of the Brillouin zone without an equivalent gap in the negative side. While observation of gaps of type A and A' had already been reported in Ref. [10], the primary result of this study is the observation of hybridization between second harmonics ($n = 2$) and the second and third zeroth-order static bands which produces the gaps labeled B and B'. Similarly to the A and A' gaps, the gaps B and B' form only on one side of the Brillouin zone and in particular on its negative side. This phenomenon is where frequency as a function of wave number $\nu(k) \neq \nu(-k)$ has been called spectral nonreciprocity [19].

The A, A' asymmetric gaps of the type observed here are known to lead to an unconventional topology of the bulk longitudinal modes in the temporally and spatially modulated systems [9]. Similarly, the B and B' asymmetric gaps will also result in longitudinal modes with nonconventional topology. The asymmetric band structure is characteristic of systems with broken parity and time-reversal symmetry [9]. At frequencies within the gaps, bulk modes can only propagate in one direction, that is, they possess nonreciprocity in their direction of propagation. In Ref. [9] we used the finite difference time domain (FDTD) method to investigate the transmission spectrum of a finite system with a sinusoidal modulation. The system was simulated by applying a treadmilling spatiotemporal modulation onto a finite system. The relation between the band structure and transmission can be understood as follows. First we consider a forward wave ($+k$) with a frequency falling with the range of gap A that propagates from a homogeneous region through a region subjected to the spatiotemporal modulation. The corresponding mode with wave number $-k$ has a negative group velocity and will be reflected by the modulated region. A wave propagating in the backward direction ($-k$) has then a positive group velocity which leads to transmission. Since the B and B' gaps

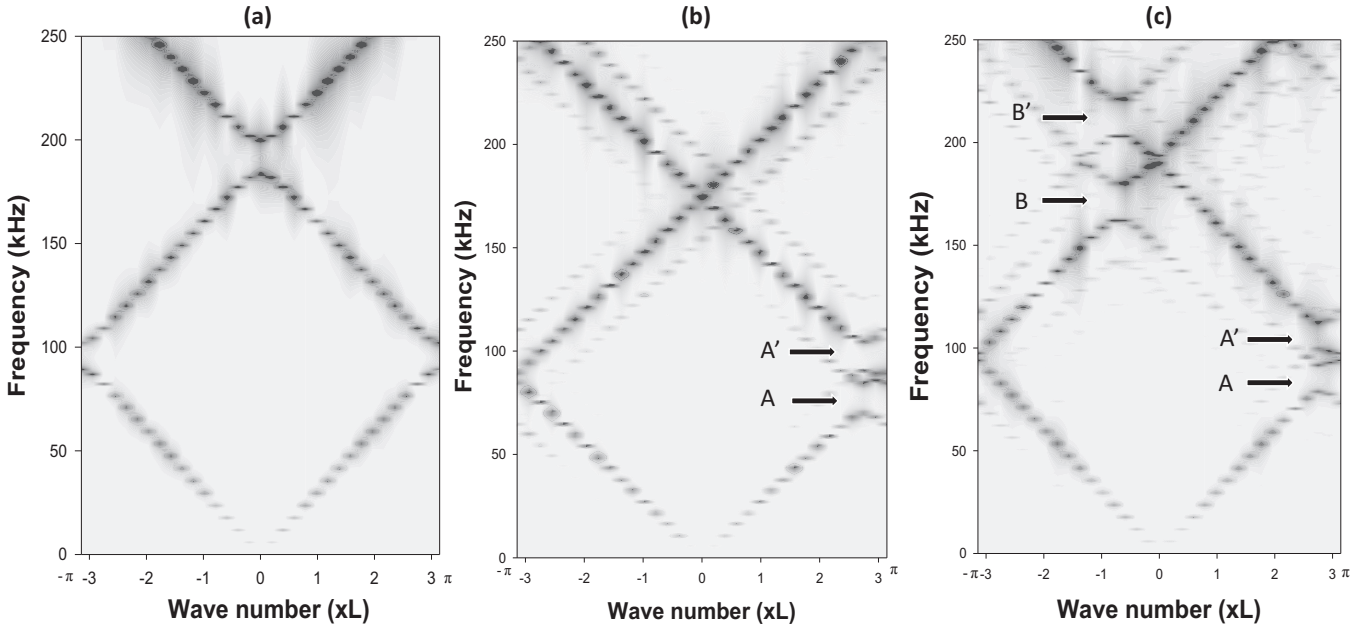

FIG. 4. Elastic band structures induced as a result of scattering by (a) static periodic Gaussian modulation, (b) moving modulation composed of a single sinusoidal function $\beta_n^{(2)}$ with the same spatial period as $\beta_n^{(1)}$, and (c) moving modulation $\beta_n^{(3)}$ composed of the first three sinusoidal Fourier components of $\beta_n^{(1)}$. To enhance the contrast, the contour plots represent the SED intensity at the power 1/400. Frequency is in kHz and wave number is in units of L.

appear on the other side of the Brillouin zone relative to the A and A' gaps, transmission and reflection of elastic waves in the B and B' frequency range will occur in the opposite direction of what was observed for the A and A' gaps. Of course nonreciprocity is not complete as a small amount of transmission (reflection) will occur due to the harmonic modes. Because of the nonreciprocity, modes with frequencies lying in the A, A' gaps showed immunity to backscattering by a mass defect embedded the region subjected to the spatiotemporal modulation [9]. The B, B'gaps will also possess immunity to back scattering but in the opposite direction to A and A'.

We now provide an explanation for the observation of B and B' hybridization gaps between second-order Stokes and anti-Stokes modes and zeroth-order modes.

Figure 4(a) is characteristic of the band structure of a superlattice that does not evolve in time. It consists of the usual folded bands of 1D periodic systems with Bragg gaps opening at the edges of the Brillouin zone and at the wave number origin. We note that the SED is less intense at the low frequency due to poor sampling of long-wavelength modes in the MD simulation of a finite length system. Figures 4(b) and 4(c) are band structures corresponding to the truncated modulations $\beta_n^{(2)}$ and $\beta_n^{(3)}$, moving with the same velocity $V = 350\,\mathrm{m/s}$.

In Fig. 4(b), the band structure of the system with the $\beta_n^{(2)}$ spatiotemporal modulation only shows the A and A' gaps and not the B and B' gaps. We recall that this modulation has the same period and velocity as the general Gaussian modulation but contains only the sinusoidal function $\sin(\frac{2\pi}{L}x_n)$. Figure 4(c) shows that when one approximates the Gaussian periodic modulation with a Fourier-like series of sinusoidal functions at several orders: $\sin(\frac{2\pi}{L}x_n)$, $\cos(2\frac{2\pi}{L}x_n)$, and $\sin(3\frac{2\pi}{L}x_n)$, one recovers the features A, A' and more importantly B, B'. The gaps B and B' arise from a mixing of different Fourier components of the Gaussian modulation. This mixing can be understood by considering a model of propagation of longitudinal waves in a one-dimensional medium subjected to a spatiotemporal modulation of its stiffness $C(x,t)$ that is the superposition of two sinusoidal functions. In the long-wavelength limit, the propagation of longitudinal elastic waves obeys the following equation of motion:

$$\rho\frac{\partial^2 u(x,t)}{\partial t^2} = \frac{\partial}{\partial x}\left(C(x,t)\frac{\partial u(x,t)}{\partial x}\right). \tag{4}$$

In Eq. (4), $u(x,t)$ is the displacement field and ρ is the mass density of the medium. Here the variation of the stiffness contains the superposition of two sinusoidal functions of position and time:

$$C(x,t) = C_0 + 2C_1\sin(K_1x + \Omega t) + 2C_2\sin(K_2x + \Omega t), \tag{5}$$

where C_0, C_1, and C_2 are positive constants. $K_i = \frac{2\pi}{L_i}$, where L_i is the period of the stiffness modulation $i = 1,2$. The frequency Ω is associated with the velocity of the stiffness modulations V. We emphasize that the two modulations possess the same velocity. The quantities K_i are independent of V. The sign of Ω determines the direction of propagation of the modulations. We now assume that the K_i values and the associated periods are related through $L_2 = L_1/2$ (i.e., $K_2 = 2K_1$). This model is equivalent to an expansion of the general modulation in terms of the first two terms in Eq. (3). In Eq. (5), for the sake of simplicity, the second-order term is chosen to be a sine function instead of the cosine function in Eq. (3). These modulations therefore only differ to a global phase which does not impact the outcomes of the analytical model.

The periodicity of the modulated one-dimensional medium $L = L_1 = 2L_2$ suggests that we should be seeking solutions

of Eq. (4) in the form of Bloch waves:

$$u(x,t) = \sum_k \sum_g u(k,g,t) e^{i(k+g)x}, \tag{6}$$

where $x \in [0,L]$. The wave number k is limited to the first Brillouin zone $[\frac{-\pi}{L}, \frac{\pi}{L}]$ and $g = \frac{2\pi}{L} m$ with m being a positive or negative integer. With this choice of form for the solution and inserting Eq. (6) into Eq. (4), the equation of propagation becomes

$$\begin{aligned}
&\frac{\partial^2 u(k+g,t)}{\partial t^2} + v_a^2 (k+g)^2 u(k+g,t) \\
&= i\varepsilon \{ f_1(k+g-K_1) u(k+g-K_1,t) e^{+i\Omega t} \\
&\quad + \alpha f_2(k+g-K_2) u(k+g-K_2,t) e^{i\Omega t} \\
&\quad + h_1(k+g+K_1) u(k+g+K_1,t) e^{-i\Omega t} \\
&\quad + \alpha h_2(k+g+K_2) u(k+g+K_2,t) e^{-i\Omega t} \},
\end{aligned} \tag{7}$$

where $f_1(k) = K_1 k + k^2$, $f_2(k) = K_2 k + k^2$, $h_1(k) = K_1 k - k^2$, $h_2(k) = K_2 k - k^2$. In Eq. (7) we have defined $v_a^2 = \frac{C_0}{\rho}$ and $\varepsilon = \frac{C_1}{\rho}$. Furthermore, we have introduced the ratio $\alpha = \frac{C_2}{C_1}$. The analysis of Eq. (7) is conducted within the framework of multiple time scale perturbation theory [22]. To explain the main result of this paper, namely the observation of the B and B' gaps, the analysis has to be conducted up to fourth order in perturbation. Details of this analysis are given in the Appendix. Here we summarize the important results that provide insight into the origin of the features observed in the band structures of Fig. 3 and in particular the emergence of the gaps B and B'.

To zeroth order in perturbation, we obtain the usual dispersion relation $\omega_0^2 = v_a^2 (k+g)^2$ correspodning to folded bands. To first order in perturbation, we find particular solutions of the form $e^{i[\omega_0(k+g\mp K_1)\pm\Omega]\tau_0}$, $e^{i[\omega_0(k+g\mp K_2)\pm\Omega]\tau_0}$. These particular solutions correspond to the first-order ($n=1$) Brillouin harmonics observed in the band structures of Figs. 3, 4(b), and 4(c). The second-order expansion leads to a correction to the zeroth-order dispersion relation:

$$\begin{aligned}
\delta\omega_0(k+g) = \frac{\varepsilon^2}{2\omega_0(k+g)} \Bigg\{ &\frac{f_1(k+g-K_1) h_1(k+g)}{\omega_0^2(k+g-K_1) - [\omega_0(k+g)-\Omega]^2} + \frac{\alpha f_2(k+g-K_2) h_2(k+g)}{\omega_0^2(k+g-K_2) - [\omega_0(k+g)-\Omega]^2} \\
&+ \frac{h_1(k+g+K_1) f_1(k+g)}{\omega_0^2(k+g+K_1) - [\omega_0(k+g)+\Omega]^2} + \frac{\alpha h_2(k+g+K_2) f_2(k+g)}{\omega_0^2(k+g+K_2) - [\omega_0(k+g)+\Omega]^2} \Bigg\}
\end{aligned}$$

This frequency shift is the signature of the formation of hybridization band gaps between the zeroth-order modes and the first Brillouin harmonics at the resonance wave numbers. The denominators of the resonance conditions: $\omega_0^2(k') - [\omega_0(k'+g)-\Omega]^2 = 0$ and $\omega_0^2(k'') - [\omega_0(k''+g)+\Omega]^2 = 0$ with $k' = k+g-K$ and $k'' = k+g+K$, determine the location of the formation of the two hybridization gaps A and A' observed in Fig. 3(d). For instance, in the case of $K = K_1$, these conditions predict hybridization gaps where the lowest zeroth-order dispersion branch ($g=0$) and the branch ($g = -\frac{2\pi}{L}$) intersect a first-order harmonic Brillouin mode. The two gaps form only on one side (positive or negative side) of the first Brillouin zone depending on the sign of Ω (i.e., the direction of propagation of the modulation of the stiffness) (see Fig. 5). These two gaps occur at the same wave number k_g. As already noted, this leads to a band structure that does not possess mirror symmetry about the frequency axis. For $K = K_2$, hybridization gaps may occur at higher frequencies outside the range reported in Figs. 3 and 4.

The particular solutions to second order in perturbation contain terms of the form $e^{i[\omega_0(k+g\mp K_1\mp K_2)\pm 2\Omega]\tau_0}$, $e^{i[\omega_0(k+g\mp 2K_1)\pm 2\Omega]\tau_0}$, $e^{i[\omega_0(k+g\mp 2K_2)\pm 2\Omega]\tau_0}$ which correspond to second harmonic Brillouin modes. To third order in perturbation, third-order harmonics appear. These are of the form $e^{i[\omega_0(k+g-2K_1-K_2)+3\Omega]\tau_0}$ with varying signs combinations of 3Ω, K_1, and K_2. The third-order solution also contains terms of the form $e^{i[\omega_0(k+g+K_2)-\Omega]\tau_0}$ which when driving the fourth-order equation, leads to secular terms. Elimination of these secular terms results in a correction of the zeroth-order dispersion relation that includes additional resonant terms. Some of these resonant terms are proportional to α, that is they only arise due to a combination of effects from the two sinusoidal components of the modulation of the stiffness.

The complete set of secular driving terms proportional to α include resonances of the type

$$\frac{1}{\omega_0^2(k+g-K_1-K_2) - [\omega_0(k+g)-2\Omega]^2}, \tag{8a}$$

$$\frac{1}{\omega_0^2(k+g-2K_1) - [\omega_0(k+g)-2\Omega]^2}, \tag{8b}$$

$$\frac{1}{\omega_0^2(k+g-2K_2) - [\omega_0(k+g)-2\Omega]^2}, \tag{8c}$$

$$\frac{1}{\omega_0^2(k+g+K_1+K_2) - [\omega_0(k+g)+2\Omega]^2}, \tag{8d}$$

$$\frac{1}{\omega_0^2(k+g+2K_1) - [\omega_0(k+g)+2\Omega]^2}, \tag{8e}$$

$$\frac{1}{\omega_0^2(k+g+2K_2) - [\omega_0(k+g)+2\Omega]^2}. \tag{8f}$$

These resonances can correct the dispersion relation in an asymmetric way and may lead to asymmetric band gaps within the Brillouin zone resulting from hybridization between a zeroth-order mode and second Brillouin harmonic bands shifted in frequency by 2Ω. The gaps labeled B and B' in Figs. 3 and 4 result from the resonance conditions (8b) and (8e) (see Fig. 5). Because $K_2 > K_1$, the other resonance conditions may lead to gaps at frequencies higher than the range of frequencies studied in this paper.

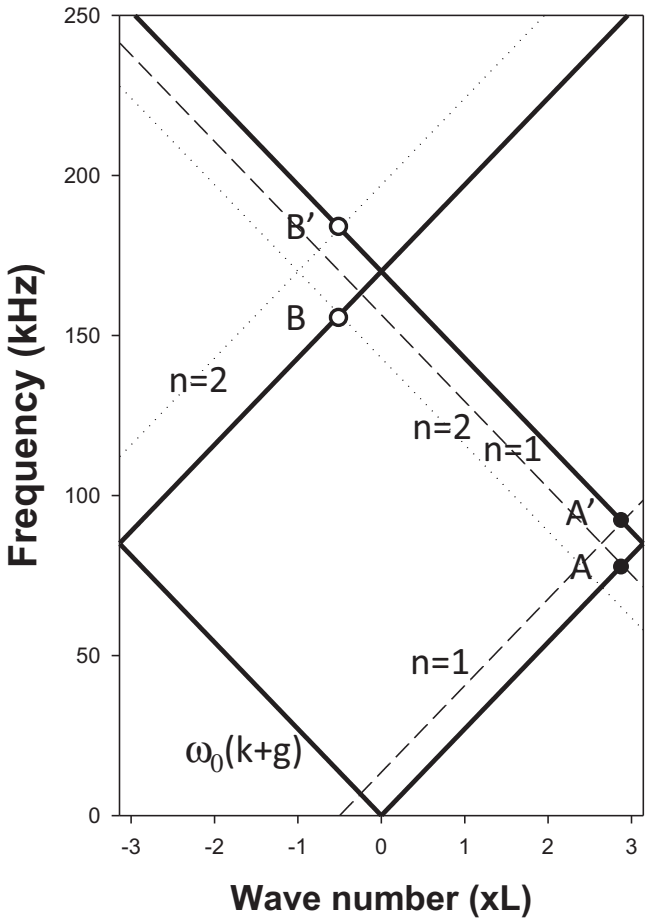

FIG. 5. Schematic illustration of the band structure of the static superlattice and of the Brillouin harmonic bands involved in the formation of the hybridization gaps A and A', and B and B'. The gap A is formed at the intersection of $\omega_0(k)$ and $\omega_0(k-K_1)-\Omega$ (i.e., when $g=0$). The gap A' forms at the intersection of $\omega_0(k-\frac{2\pi}{L})$ and $\omega_0(k-\frac{2\pi}{L}+K_1)+\Omega=\omega_0(k)+\Omega$ (i.e., when $g=-\frac{2\pi}{L}$). The gaps B and B' are occurring where the conditions $\omega_0^2(k+g-2K_1)-[\omega_0(k+g)-2\Omega]^2$ and $\omega_0^2(k+g+2K_1)-[\omega_0(k+g)+2\Omega]^2$ are satisfied. The B point is the intersection between $\omega_0(k-\frac{2\pi}{L}+2K_1)=\omega_0(k+\frac{2\pi}{L})$ and $\omega_0(k-\frac{2\pi}{L})-2\Omega$. The B' point is the intersection between $\omega_0(k+\frac{2\pi}{L}-2K_1)=\omega_0(k-\frac{2\pi}{L})$ and $\omega_0(k+\frac{2\pi}{L})+2\Omega$.

In this theoretical analysis, we limited ourselves to the interaction between two sinusoidal components of the spatiotemporal modulation of stiffness. Other hybridization modes will arise from a combination of additional sinusoidal functions in the expansion of a general periodic function. The content of a Fourier series representing some general periodic modulation of stiffness can therefore be viewed as a means of designing specific symmetry breaking features in the band structure of an elastic material.

IV. CONCLUSIONS

We have demonstrated the significant effect of changing the shape of spatiotemporal stiffness modulation on the nonreciprocal band structure of elastic waves propagating in a one-dimensional elastic medium. A spatial modulation composed of periodic arrangements of Gaussian functions leads to a number of features in the elastic band structure that include harmonic modes reminiscent of Brillouin scattering and hybridization band gaps. The hybridization gaps result from interactions between the Bloch modes of the medium subjected to the static modulation and the sinusoidal components of the Fourier decomposition of the modulation. We show with a theoretical model that two Fourier components of some general periodic modulation can combine to lead to new gaps that were not present when considering a single sinusoidal modulation. Shaping the spatiotemporal modulations of stiffness can then be employed as a tool for elastic band structure design, i.e., designing specific symmetry breaking band features. This concept vindicates the notion of functional on-demand elastic materials. By deliberately modifying material's properties (e.g., stiffness) using an external and contact or noncontact stimulating field we can envision the possibility of creating on-demand writable and rewritable artificial "microstructures" through spatiotemporal modulations. Rewritable microstructures extend the geometric scale and dynamic range of the conventional arrangement of "phases", "interfaces, and defects" that a material can support by overcoming thermodynamics and kinetic microstructural constraints. By combining spatiotemporal control with intrinsic materials properties, we enable the creation of on-demand functions than can be programmed into—and elicited from—a material's microstructure topography and time evolution. Such an approach extends the realm of materials properties far beyond those achievable with conventional materials microstructural design. Using the dynamic coupling between the programmed microstructure and individual materials properties (e.g., photonic, electronic, phononic, magnonic, etc.) as a steering wheel, offers a vast array of pathways to access by design: materials with broken symmetry (time reversal, parity, chiral, particle-hole), new topological classes of materials, Dirac materials, the controlled transport reciprocity and manipulation of electron, photon, and phonon trajectories in materials.

ACKNOWLEDGMENT

We acknowledge financial support from NSF Award No. 1640860.

APPENDIX

For the sake of analytical simplicity in the context of multiple time scale perturbation theory, we treat ε in Eq. (7) as a perturbation and write the displacement as a fourth-order power series in the perturbation, namely

$$u(k+g,\ \tau_0,\tau_1,\tau_2,\tau_3,\tau_4)=u_0(k+g,\ \tau_0,\tau_1,\tau_2,\tau_3,\tau_4)+\varepsilon u_1(k+g,\ \tau_0,\tau_1,\tau_2,\tau_3,\tau_4)+\varepsilon^2 u_2(k+g,\ \tau_0,\tau_1,\tau_2,\tau_3,\tau_4)$$
$$+\varepsilon^3 u_3(k+g,\ \tau_0,\tau_1,\tau_2,\tau_3,\tau_4)+\varepsilon^4 u_4(k+g,\ \tau_0,\tau_1,\tau_2,\tau_3,\tau_4). \quad \text{(A1)}$$

In Eq. (A1), u_i with $i = 0,1,2,3,4$ are displacement functions expressed to zeroth, first, second, third and fourth order in the perturbation. We have also replaced the single time variable t by five variables representing different time scales: $\tau_n = \varepsilon^n t = \varepsilon^n \tau_0$ with $n = 0,1,2,3,4$. We can subsequently decompose Eq. (7) into five equations: one equation to zeroth order in ε, one equation to first order in ε, a third equation to second order in ε, a fourth equation to third order in ε, and a fifth equation to fourth order in ε.

The zeroth-order equation:

$$\frac{\partial^2 u_0(k+g,\tau_0,\tau_1,\tau_2,\tau_3,\tau_4)}{\partial \tau_0^2} + v_a^2(k+g)^2 u_0(k+g,\tau_0,\tau_1,\tau_2,\tau_3,\tau_4) = 0 \tag{A2}$$

has solution

$$u_0(k+g,\tau_0,\tau_1,\tau_2,\tau_3,\tau_4) = a_0(k+g,\tau_1,\tau_2,\tau_3,\tau_4)e^{i\omega_0(k+g)\tau_0}, \tag{A3a}$$

with the eigenvalue

$$\omega_0^2 = v_a^2(k+g)^2. \tag{A3b}$$

To first order, the equation of motion is

$$\begin{aligned}
&\frac{\partial^2 u_1(k+g,\tau_0,\tau_1,\tau_2,\tau_3,\tau_4)}{\partial \tau_0^2} + 2\frac{\partial^2 u_0(k+g,\tau_0,\tau_1,\tau_2,\tau_3,\tau_4)}{\partial \tau_1 \partial \tau_0} + v_a^2(k+g)^2 u_1(k+g,\tau_0,\tau_1,\tau_2,\tau_3,\tau_4) \\
&= i\{f_1(k+g-K_1)u_0(k+g-K_1,t)e^{+i\Omega\tau_0} + \alpha f_2(k+g-K_2)u_0(k+g-K_2,t)e^{i\Omega\tau_0} \\
&\quad + h_1(k+g+K_1)u_0(k+g+K_1,t)e^{-i\Omega\tau_0} + \alpha h_2(k+g+K_2)u_0(k+g+K_2,t)e^{-i\Omega\tau_0}\}.
\end{aligned} \tag{A4}$$

Inserting the zeroth-order solution [Eq. (A3a)] into Eq. (A4) will make the second term on the right-hand side of the equation lead to a secular term. We eliminate this term by making u_0 independent of τ_1. Subsequently, we will make displacements at all order independent of τ_1. In anticipation of the appearance of similar secular terms in the fourth-order equation of motion, we will also make all displacements independent of τ_3. In fact, we eliminate dependencies on the time scales with odd powers of ε.

With this, the solution of Eq. (A4) is composed of a homogeneous solution and a particular solution:

$$\begin{aligned}
u_1(k+g,\tau_0,\tau_2,\tau_4) &= u_{1,H}(k+g,\tau_0,\tau_2,\tau_4) + u_{1,P}(k+g,\tau_0,\tau_2,\tau_4) \\
&= a_1(k+g,\tau_2,\tau_4)e^{i\omega_0(k+g)\tau_0} + i\frac{f_1(k+g-K_1)a_0(k+g-K_1,\tau_2,\tau_4)}{\omega_0^2(k+g) - [\omega_0(k+g-K_1)+\Omega]^2}e^{i[\omega_0(k+g-K_1)+\Omega]\tau_0} \\
&\quad + i\frac{\alpha f_2(k+g-K_2)a_0(k+g-K_2,\tau_2,\tau_4)}{\omega_0^2(k+g) - [\omega_0(k+g-K_2)+\Omega]^2}e^{i[\omega_0(k+g-K_2)+\Omega]\tau_0} \\
&\quad + i\frac{h_1(k+g+K_1)a_0(k+g+K_1,\tau_2,\tau_4)}{\omega_0^2(k+g) - [\omega_0(k+g+K_1)-\Omega]^2}e^{i[\omega_0(k+g+K_1)-\Omega]\tau_0} \\
&\quad + i\frac{\alpha h_2(k+g+K_2)a_0(k+g+K_2,\tau_2,\tau_4)}{\omega_0^2(k+g) - [\omega_0(k+g+K_2)-\Omega]^2}e^{i[\omega_0(k+g+K_2)-\Omega]\tau_0}.
\end{aligned} \tag{A5}$$

Note that the fractions in Eq. (A5) may diverge. One may add a small imaginary term (damping) to the denominators to eliminate the divergence. The zero limit of the imaginary term would be eventually taken. For the sake of presenting the most compact equations, we have elected in the subsequent derivations to omit this damping term.

To second order, the equation of motion takes the form

$$\begin{aligned}
&\frac{\partial^2 u_2(k+g,\tau_0,\tau_2,\tau_4)}{\partial \tau_0^2} + 2\frac{\partial^2 u_0(k+g,\tau_0,\tau_2,\tau_4)}{\partial \tau_2 \partial \tau_0} + v_a^2(k+g)^2 u_2(k+g,\tau_0,\tau_2,\tau_4) \\
&= i\{f_1(k+g-K_1)u_1(k+g-K_1,\tau_0,\tau_2,\tau_4)e^{i\Omega\tau_0} + \alpha f_2(k+g-K_2)u_1(k+g-K_2,\tau_0,\tau_2,\tau_4)e^{i\Omega\tau_0} \\
&\quad + h_1(k+g+K_1)u_1(k+g+K_1,\tau_0,\tau_2,\tau_4)e^{-i\Omega\tau_0} + \alpha h_2(k+g+K_2)u_1(k+g+K_2,\tau_0,\tau_2,\tau_4)e^{-i\Omega\tau_0}\}.
\end{aligned} \tag{A6}$$

We need to insert Eq. (A5) into Eq. (A6). Equation (A6) is separated into two equations. The first equation is used to eliminate secular terms:

$$
\begin{aligned}
&2\frac{\partial^2 u_0(k+g,\tau_0,\tau_2,\tau_4)}{\partial\tau_2\partial\tau_0}\\
&\quad=-\frac{f_1(k+g-K_1)h_1(k+g)a_0(k+g,\tau_2,\tau_4)}{\omega_0^2(k+g-K_1)-(\omega_0(k+g)-\Omega)^2}e^{i\omega_0(k+g)\tau_0}-\frac{\alpha f_2(k+g-K_2)h_2(k+g)a_0(k+g,\tau_2,\tau_4)}{\omega_0^2(k+g-K_2)-(\omega_0(k+g)-\Omega)^2}e^{i\omega_0(k+g)\tau_0}\\
&\quad\quad-\frac{h_1(k+g+K_1)f_1(k+g)a_0(k+g,\tau_2,\tau_4)}{\omega_0^2(k+g+K_1)-(\omega_0(k+g)+\Omega)^2}e^{i\omega_0(k+g)\tau_0}-\frac{\alpha h_2(k+g+K_2)f_2(k+g)a_0(k+g,\tau_2,\tau_4)}{\omega_0^2(k+g+K_2)-(\omega_0(k+g)+\Omega)^2}e^{i\omega_0(k+g)\tau_0}.
\end{aligned}
\tag{A7}
$$

This equation will lead to a second-order correction to the zeroth-order eigenvalue [Eq. (A3b)]. To do this, we express the zeroth-order amplitude in the complex form $a_0(k+g,\tau_4)=\alpha_0(\tau_4)e^{i\varphi(k+g)\tau_2}$. With this $u_0(k+g,\tau_0,,\tau_2,\tau_4)=\alpha_0(\tau_4)e^{i\omega_0(k+g)\tau_0}e^{i\varphi(k+g)\tau_2}=\alpha_0(\tau_4)e^{i[\omega_0(k+g)+\varphi(k+g)\varepsilon^2]\tau_0}=\alpha_0(\tau_4)e^{i\omega_0^*(k+g)\tau_0}$.

Then one obtains a correction to $\omega_0(k+g)$, leading to a frequency shift and damping. This frequency shift is most pronounced for values of the wave number leading to strong resonances and is given by

$$
\begin{aligned}
\delta\omega_0(k+g)&=\omega_0^*(k+g)-\omega_0(k+g)=\varepsilon^2\varphi\\
&=\frac{\varepsilon^2}{2\omega_0(k+g)}\left\{\frac{f_1(k+g-K_1)h_1(k+g)}{\omega_0^2(k+g-K_1)-[\omega_0(k+g)-\Omega]^2}+\frac{\alpha f_2(k+g-K_2)h_2(k+g)}{\omega_0^2(k+g-K_2)-[\omega_0(k+g)-\Omega]^2}\right.\\
&\quad\left.+\frac{h_1(k+g+K_1)f_1(k+g)}{\omega_0^2(k+g+K_1)-[\omega_0(k+g)+\Omega]^2}+\frac{\alpha h_2(k+g+K_2)f_2(k+g)}{\omega_0^2(k+g+K_2)-[\omega_0(k+g)+\Omega]^2}\right\}.
\end{aligned}
\tag{A8}
$$

The second-order equation takes the form

$$
\frac{\partial^2 u_2(k+g,\tau)}{\partial\tau_0^2}+v_a^2(k+g)^2u_2(k+g,\tau)=A_1+A_2+A_3+A_4,
\tag{A9}
$$

where

$$
\begin{aligned}
A_1=\{&if_1(k+g-K_1)a_1(k+g-K_1,\tau)e^{i[\omega_0(k+g-K_1)+\Omega]\tau_0}+i\alpha f_2(k+g-K_2)a_1(k+g-K_2,\tau)e^{i[\omega_0(k+g-K_2)+\Omega]\tau_0}\\
&+ih_1(k+g+K_1)a_1(k+g+K_1,\tau)e^{i[\omega_0(k+g+K_1)-\Omega]\tau_0}+i\alpha h_2(k+g+K_2)a_1(k+g+K_2,\tau)e^{i[\omega_0(k+g+K_2)-\Omega]\tau_0}\}
\end{aligned}
$$

and

$$
\begin{aligned}
A_2=\Bigg\{&-\frac{f_1(k+g-K_1)\alpha h_2(k+g-K_1+K_2)a_0(k+g-K_1+K_2,\tau)}{\omega_0^2(k+g-K_1)-[\omega_0(k+g-K_1+K_2)-\Omega]^2}e^{i(\omega_0(k+g-K_1+K_2))\tau_0}\\
&-\frac{\alpha h_2(k+g+K_2)f_1(k+g-K_1+K_2)a_0(k+g-K_1+K_2,\tau)}{\omega_0^2(k+g+K_2)-(\omega_0(k+g-K_1+K_2)+\Omega)^2}e^{i(\omega_0(k+g-K_1+K_2))\tau_0}\\
&-\frac{\alpha f_2(k+g-K_2)h_1(k+g+K_1-K_2)a_0(k+g+K_1-K_2,\tau)}{\omega_0^2(k+g-K_2)-(\omega_0(k+g+K_1-K_2)-\Omega)^2}e^{i(\omega_0(k+g+K_1-K_2))\tau_0}\\
&-\frac{h_1(k+g+K_1)\alpha f_2(k+g+K_1-K_2)a_0(k+g+K_1-K_2,\tau)}{\omega_0^2(k+g+K_1)-(\omega_0(k+g+K_1-K_2)+\Omega)^2}e^{i(\omega_0(k+g+K_1-K_2))\tau_0}\Bigg\}
\end{aligned}
$$

and

$$
\begin{aligned}
A_3=\Bigg\{&-\frac{f_1(k+g-K_1)\alpha f_2(k+g-K_1-K_2)a_0(k+g-K_1-K_2,\tau)}{\omega_0^2(k+g-K_1)-(\omega_0(k+g-K_1+K_2)+\Omega)^2}e^{i(\omega_0(k+g-K_1-K_2)+2\Omega)\tau_0}\\
&-\frac{\alpha f_2(k+g-K_2)f_1(k+g-K_1-K_2)a_0(k+g-K_1-K_2,\tau)}{\omega_0^2(k+g-K_2)-(\omega_0(k+g-K_1-K_2)+\Omega)^2}e^{i(\omega_0(k+g-K_1-K_2)+2\Omega)\tau_0}\\
&-\frac{f_1(k+g-K_1)f_1(k+g-2K_1)a_0(k+g-2K_1,\tau)}{\omega_0^2(k+g-K_1)-(\omega_0(k+g-2K_1)+\Omega)^2}e^{i(\omega_0(k+g-2K_1)+2\Omega)\tau_0}\\
&-\frac{\alpha f_2(k+g-K_2)\alpha f_2(k+g-2K_2)a_0(k+g-2K_2,\tau)}{\omega_0^2(k+g-K_2)-(\omega_0(k+g-2K_2)+\Omega)^2}e^{i(\omega_0(k+g-2K_2)+2\Omega)\tau_0}\Bigg\}
\end{aligned}
$$

and

$$A_4 = \Bigg\{ -\frac{h_1(k+g+K_1)\alpha h_2(k+g+K_1+K_2)a_0(k+g+K_1+K_2,\tau)}{\omega_0^2(k+g+K_1)-(\omega_0(k+g+K_1+K_2)-\Omega)^2} e^{i(\omega_0(k+g+K_1+K_2)-2\Omega)\tau_0}$$
$$- \frac{\alpha h_2(k+g+K_2)h_1(k+g+K_1+K_2)a_0(k+g+K_1+K_2,\tau)}{\omega_0^2(k+g+K_2)-(\omega_0(k+g+K_1+K_2)-\Omega)^2} e^{i(\omega_0(k+g+K_1+K_2)-2\Omega)\tau_0}$$
$$- \frac{h_1(k+g+K_1)h_1(k+g+2K_1)a_0(k+g+2K_1,\tau)}{\omega_0^2(k+g+K_1)-(\omega_0(k+g+2K_1)-\Omega)^2} e^{i(\omega_0(k+g+2K_1)-2\Omega)\tau_0}$$
$$- \frac{\alpha h_2(k+g+K_2)\alpha h(k+g+2K_2)a_0(k+g+2K_2,\tau)}{\omega_0^2(k+g+K_2)-(\omega_0(k+g+2K_2)-\Omega)^2} e^{i(\omega_0(k+g+2K_2)-2\Omega)\tau_0} \Bigg\}.$$

For the sake of compactness, in the preceding relations we have replaced the dependency on τ_0, τ_2, τ_4 by a single symbol τ. We now seek the solution of Eq. (A9) in the form of the sum of a homogenous part and a particular part:

$$u_2 = u_{2,H} + u_{2,P}. \tag{A10}$$

The homogenous solution is

$$u_{2,H}(k+g,\tau) = a_2(k+g,\tau)e^{i\omega_0(k+g)\tau_0}.$$

The particular solution $u_{2,p}$ includes several parts arising from the driving terms A_1, A_2, A_3, and A_4. The term A_1 leads to the following contributions to the particular solution:

$$u_{2,p}^{(1)} = \Bigg\{ \frac{1}{\omega_0^2(k+g)-(\omega_0(k+g-K_1)+\Omega)^2} i f_1(k+g-K_1)a_1(k+g-K_1,\tau)e^{i(\omega_0(k+g-K_1)+\Omega)\tau_0}$$
$$+ \frac{1}{\omega_0^2(k+g)-(\omega_0(k+g-K_2)+\Omega)^2} i\alpha f_2(k+g-K_2)a_1(k+g-K_2,\tau)e^{i(\omega_0(k+g-K_2)+\Omega)\tau_0}$$
$$+ \frac{1}{\omega_0^2(k+g)-(\omega_0(k+g+K_1)-\Omega)^2} i h_1(k+g+K_1)a_1(k+g+K_1,\tau)e^{i(\omega_0(k+g+K_1)-\Omega)\tau_0}$$
$$+ \frac{1}{\omega_0^2(k+g)-(\omega_0(k+g+K_2)-\Omega)^2} i\alpha h_2(k+g+K_2)a_1(k+g+K_2,\tau)e^{i(\omega_0(k+g+K_2)-\Omega)\tau_0} \Bigg\}.$$

The term A_2 leads to the following contributions to the particular solution:

$$u_{2,p}^{(2)} = \frac{1}{\omega_0^2(k+g)-\omega_0^2(k+g-K_1+K_2)} \Bigg\{ -\frac{f_1(k+g-K_1)\alpha h_2(k+g-K_1+K_2)a_0(k+g-K_1+K_2,\tau)}{\omega_0^2(k+g-K_1)-(\omega_0(k+g-K_1+K_2)-\Omega)^2}$$
$$- \frac{\alpha h_2(k+g+K_2)f_1(k+g-K_1+K_2)a_0(k+g-K_1+K_2,\tau)}{\omega_0^2(k+g+K_2)-(\omega_0(k+g-K_1+K_2)+\Omega)^2} \Bigg\} e^{i(\omega_0(k+g-K_1+K_2))\tau_0}$$
$$+ \frac{1}{\omega_0^2(k+g)-\omega_0^2(k+g+K_1-K_2)} \Bigg\{ -\frac{\alpha f_2(k+g-K_2)h_1(k+g+K_1-K_2)a_0(k+g+K_1-K_2,\tau)}{\omega_0^2(k+g-K_2)-(\omega_0(k+g+K_1-K_2)-\Omega)^2}$$
$$- \frac{h_1(k+g+K_1)\alpha f_2(k+g+K_1-K_2)a_0(k+g+K_1-K_2,\tau)}{\omega_0^2(k+g+K_1)-(\omega_0(k+g+K_1-K_2)+\Omega)^2} \Bigg\} e^{i(\omega_0(k+g+K_1-K_2))\tau_0}.$$

The term A_3 gives

$$u_{2,p}^{(3)} = \frac{1}{\omega_0^2(k+g)-(\omega_0(k+g-K_1-K_2)+2\Omega)^2} \Bigg\{ -\frac{f_1(k+g-K_1)\alpha f_2(k+g-K_1-K_2)a_0(k+g-K_1-K_2,\tau)}{\omega_0^2(k+g-K_1)-(\omega_0(k+g-K_1-K_2)+\Omega)^2}$$
$$- \frac{\alpha f_2(k+g-K_2)f_1(k+g-K_1-K_2)a_0(k+g-K_1-K_2,\tau)}{\omega_0^2(k+g-K_2)-(\omega_0(k+g-K_1-K_2)+\Omega)^2} \Bigg\} e^{i(\omega_0(k+g-K_1-K_2)+2\Omega)\tau_0}$$
$$- \frac{1}{\omega_0^2(k+g)-(\omega_0(k+g-2K_1)+2\Omega)^2} \frac{f_1(k+g-K_1)f_1(k+g-2K_1)a_0(k+g-2K_1,\tau)}{\omega_0^2(k+g-K_1)-(\omega_0(k+g-2K_1)+\Omega)^2} e^{i(\omega_0(k+g-2K_1)+2\Omega)\tau_0}$$
$$- \frac{1}{\omega_0^2(k+g)-(\omega_0(k+g-2K_2)+2\Omega)^2} \frac{\alpha f_2(k+g-K_2)\alpha f_2(k+g-2K_2)a_0(k+g-2K_2,\tau)}{\omega_0^2(k+g-K_2)-(\omega_0(k+g-2K_2)+\Omega)^2} e^{i(\omega_0(k+g-2K_2)+2\Omega)\tau_0}.$$

The term A_4 leads to

$$u^{(4)}_{2,p} = \frac{1}{\omega_0^2(k+g)-(\omega_0(k+g+K_1+K_2)-2\Omega)^2}\left\{-\frac{h_1(k+g+K_1)\alpha h_2(k+g+K_1+K_2)a_0(k+g+K_1+K_2,\tau)}{\omega_0^2(k+g+K_1)-(\omega_0(k+g+K_1+K_2)-\Omega)^2}\right.$$
$$\left.-\frac{\alpha h_2(k+g+K_2)h_1(k+g+K_1+K_2)a_0(k+g+K_1+K_2,\tau)}{\omega_0^2(k+g+K_2)-(\omega_0(k+g+K_1+K_2)-\Omega)^2}\right\}e^{i(\omega_0(k+g+K_1+K_2)-2\Omega)\tau_0}$$
$$-\frac{1}{\omega_0^2(k+g)-(\omega_0(k+g+2K_1)-2\Omega)^2}\frac{h_1(k+g+K_1)h_1(k+g+2K_1)a_0(k+g+2K_1,\tau)}{\omega_0^2(k+g+K_1)-(\omega_0(k+g+2K_1)-\Omega)^2}e^{i(\omega_0(k+g+2K_1)-2\Omega)\tau_0}$$
$$-\frac{1}{\omega_0^2(k+g)-(\omega_0(k+g+2K_2)-2\Omega)^2}\frac{\alpha h_2(k+g+K_2)\alpha h(k+g+2K_2)a_0(k+g+2K_2,\tau)}{\omega_0^2(k+g+K_2)-(\omega_0(k+g+2K_2)-\Omega)^2}e^{i(\omega_0(k+g+2K_2)-2\Omega)\tau_0}.$$

The wave equation to third order is given by

$$\frac{\partial^2 u_3(k+g,\tau)}{\partial\tau_0^2}+2\frac{\partial^2 u_1(k+g,\tau)}{\partial\tau_0\partial\tau_2}+v_a^2(k+g)^2u_3(k+g,\tau)$$
$$=i\{f_1(k+g-K_1)u_2(k+g-K_1,\tau)e^{i\Omega\tau_0}+\alpha f_2(k+g-K_2)u_2(k+g-K_2,\tau)e^{i\Omega\tau_0}$$
$$+h_1(k+g+K_1)u_2(k+g+K_1,\tau)e^{-i\Omega\tau_0}+\alpha h_2(k+g+K_2)u_2(k+g+K_2,\tau)e^{-i\Omega\tau_0}\}. \tag{A11}$$

This equation is rewritten in the form

$$\frac{\partial^2 u_3(k+g,\tau)}{\partial\tau_0^2}+2\frac{\partial^2 u_1(k+g,\tau)}{\partial\tau_0\partial\tau_2}+v_a^2(k+g)^2u_3(k+g,\tau)=i\{B_1+B_2+B_3+B_4\}.$$

We find

$$\frac{\partial^2 u_1(k+g,\tau)}{\partial\tau_0\partial\tau_2}=\frac{\partial a_1(k+g,\tau)}{\partial\tau_2}i\omega_0(k+g)e^{i\omega_0(k+g)\tau_0}+i\frac{f_1(k+g-K_1)}{\omega_0^2(k+g)-(\omega_0(k+g-K_1)+\Omega)^2}\alpha_0 i\varphi(k+g-K_1)$$
$$\times e^{i\varphi(k+g-K_1)\tau_2}i(\omega_0(k+g-K_1)+\Omega)e^{i(\omega_0(k+g-K_1)+\Omega)\tau_0}$$
$$+i\frac{\alpha f_2(k+g-K_2)}{\omega_0^2(k+g)-(\omega_0(k+g-K_2)+\Omega)^2}\alpha_0 i\varphi(k+g-K_2)e^{i\varphi(k+g-K_2)\tau_2}i(\omega_0(k+g-K_2)+\Omega)e^{i(\omega_0(k+g-K_2)+\Omega)\tau_0}$$
$$+i\frac{h_1(k+g+K_1)}{\omega_0^2(k+g)-(\omega_0(k+g+K_1)-\Omega)^2}\alpha_0 i\varphi(k+g+K_1)e^{i\varphi(k+g+K_1)\tau_2}i(\omega_0(k+g+K_1)-\Omega)e^{i(\omega_0(k+g+K_1)-\Omega)\tau_0}$$
$$+i\frac{\alpha h_2(k+g+K_2)}{\omega_0^2(k+g)-(\omega_0(k+g+K_2)-\Omega)^2}\alpha_0 i\varphi(k+g+K_2)e^{i\varphi(k+g+K_2)\tau_2}i(\omega_0(k+g+K_2)-\Omega)e^{i(\omega_0(k+g+K_2)-\Omega)\tau_0} \tag{A12}$$

We now use Eqs. (A5) and (A10) to evaluate B_1, B_2, B_3, and B_4.

We illustrate the process with the term B_1:

$$iB_1 = i f_1(k+g-K_1)u_2(k+g-K_1,\tau)e^{i\Omega\tau_0}$$
$$= i f_1(k+g-K_1)a_2(k+g-K_1,\tau)e^{i(\omega_0(k+g-K_1)+\Omega)\tau_0}+i f_1\,(k+g-K_1)$$
$$\times\left\{\frac{1}{\omega_0^2(k+g-K_1)-(\omega_0(k+g-2K_1)+\Omega)^2}i f_1(k+g-2K_1)a_1(k+g-2K_1,\tau)e^{i(\omega_0(k+g-2K_1)+2\Omega)\tau_0}\right.$$
$$+\frac{1}{\omega_0^2(k+g-K_1)-(\omega_0(k+g-K_1-K_2)+\Omega)^2}i\alpha f_2(k+g-K_1-K_2)a_1(k+g-K_1-K_2,\tau)e^{i(\omega_0(k+g-K_1-K_2)+2\Omega)\tau_0}$$
$$+\frac{1}{\omega_0^2(k+g-K_1)-(\omega_0(k+g)-\Omega)^2}ih_1(k+g)a_1(k+g,\tau)e^{i(\omega_0(k+g))\tau_0}$$
$$\left.+\frac{1}{\omega_0^2(k+g-K_1)-(\omega_0(k+g-K_1+K_2)-\Omega)^2}i\alpha h_2(k+g-K_1+K_2)a_1(k+g-K_1+K_2,\tau)e^{i(\omega_0(k+g-K_1+K_2))\tau_0}\right\}$$
$$+i f_1\,(k+g-K_1)\left\{\frac{1}{\omega_0^2(k+g-K_1)-\omega_0^2(k+g-2K_1+K_2)}\right.$$
$$\times\left\{-\frac{f_1(k+g-2K_1)\alpha h_2(k+g-2K_1+K_2)a_0(k+g-2K_1+K_2,\tau)}{\omega_0^2(k+g-2K_1)-(\omega_0(k+g-2K_1+K_2)-\Omega)^2}\right.$$

$$
\begin{aligned}
&- \frac{\alpha h_2(k+g-K_1+K_2) f_1(k+g-2K_1+K_2) a_0(k+g-2K_1+K_2,\tau)}{\omega_0^2(k+g-K_1+K_2)-(\omega_0(k+g-2K_1+K_2)+\Omega)^2}\Big\} e^{i(\omega_0(k+g-2K_1+K_2)+\Omega)\tau_0} \\
&+ \frac{1}{\omega_0^2(k+g-K_1)-\omega_0^2(k+g-K_2)} \\
&\times \Big\{ - \frac{\alpha f_2(k+g-K_1-K_2) h_1(k+g-K_2) a_0(k+g-K_2,\tau)}{\omega_0^2(k+g-K_1-K_2)-(\omega_0(k+g-K_2)-\Omega)^2} \\
&- \frac{h_1(k+g)\alpha f_2(k+g-K_2) a_0(k+g-K_2,\tau)}{\omega_0^2(k+g)-(\omega_0(k+g-K_2)+\Omega)} \Big\} e^{i(\omega_0(k+g-K_2)+\Omega)\tau_0} \Big\} \\
&+ i f_1\,(k+g-K_1) \Big\{ \frac{1}{\omega_0^2(k+g-K_1)-(\omega_0(k+g-2K_1-K_2)+2\Omega)^2} \\
&\times \Big\{ - \frac{f_1(k+g-2K_1)\alpha f_2(k+g-2K_1-K_2) a_0(k+g-2K_1-K_2,\tau)}{\omega_0^2(k+g-2K_1)-(\omega_0(k+g-2K_1+K_2)+\Omega)^2} \\
&- \frac{\alpha f_2(k+g-K_1-K_2) f_1(k+g-2K_1-K_2) a_0(k+g-2K_1-K_2,\tau)}{\omega_0^2(k+g-K_1-K_2)-(\omega_0(k+g-2K_1-K_2)+\Omega)^2} \Big\} e^{i(\omega_0(k+g-2K_1-K_2)+3\Omega)\tau_0} \\
&- \frac{1}{\omega_0^2(k+g-K_1)-(\omega_0(k+g-3K_1)+2\Omega)^2} \frac{f_1(k+g-2K_1) f_1(k+g-3K_1) a_0(k+g-3K_1,\tau)}{\omega_0^2(k+g-2K_1)-(\omega_0(k+g-3K_1)+\Omega)^2} e^{i(\omega_0(k+g-3K_1)+3\Omega)\tau_0} \\
&- \frac{1}{\omega_0^2(k+g-K_1)-(\omega_0(k+g-K_1-2K_2)+2\Omega)^2} \\
&\times \frac{\alpha f_2(k+g-K_1-K_2)\alpha f_2(k+g-K_1-2K_2) a_0(k+g-K_1-2K_2,\tau)}{\omega_0^2(k+g-K_1-K_2)-(\omega_0(k+g-K_1-2K_2)+\Omega)^2} e^{i(\omega_0(k+g-K_1-2K_2)+3\Omega)\tau_0} \Big\} \\
&+ i f_1\,(k+g-K_1) \Big\{ \frac{1}{\omega_0^2(k+g-K_1)-(\omega_0(k+g+K_2)-2\Omega)^2} \Big\{ \frac{h_1(k+g)\alpha h_2(k+g+K_2) a_0(k+g+K_2,\tau)}{\omega_0^2(k+g)-(\omega_0(k+g+K_2)-\Omega)^2} \\
&- \frac{\alpha h_2(k+g-K_1+K_2) h_1(k+g+K_2) a_0(k+g+K_2,\tau)}{\omega_0^2(k+g-K_1+K_2)-(\omega_0(k+g+K_2)-\Omega)^2} \Big\} e^{i(\omega_0(k+g+K_2)-\Omega)\tau_0} \\
&- \frac{1}{\omega_0^2(k+g-K_1)-(\omega_0(k+g+K_1)-2\Omega)^2} \frac{h_1(k+g) h_1(k+g+K_1) a_0(k+g+K_1,\tau)}{\omega_0^2(k+g)-(\omega_0(k+g+K_1)-\Omega)^2} e^{i(\omega_0(k+g+K_1)-\Omega)\tau_0} \\
&- \frac{1}{\omega_0^2(k+g-K_1)-(\omega_0(k+g-K_1+2K_2)-2\Omega)^2} \\
&\times \frac{\alpha h_2(k+g-K_1+K_2)\alpha h(k+g-K_1+2K_2) a_0(k+g-K_1+2K_2,\tau)}{\omega_0^2(k+g-K_1+K_2)-(\omega_0(k+g-K_1+2K_2)-\Omega)^2} e^{i(\omega_0(k+g-K_1+2K_2)-\Omega)\tau_0} \Big\}
\end{aligned}
$$

Similarly complex expressions will be found for the other driving terms. We note that all the secular terms of form $e^{i\omega_0(k+g)\tau_0}$ will be used to eliminate the first term on the right-hand side of Eq. (A12). We are particularly interested in driving terms with the form $e^{i(\omega_0(k^*)\pm\Omega)\tau_0}$ and resonant amplitudes with denominators of the form $\omega_0^2(k+g+K')-(\omega_0(k+g+K'')\pm 2\Omega)^2$. For instance, the term B_2 leads to terms of the form

$$
\begin{aligned}
&i\alpha f_2(k+g-K_2) \Big\{ \frac{1}{\omega_0^2(k+g-K_2)-(\omega_0(k+g+K_1)-2\Omega)^2} \Big\{ - \frac{h_1(k+g+K_1-K_2)\alpha h_2(k+g+K_1K_2) a_0(k+g+K_1,\tau)}{\omega_0^2(k+g+K_1)-(\omega_0(k+g+K_1+K_2)-\Omega)^2} \\
&- \frac{\alpha h_2(k+g) h_1(k+g+K_1) a_0(k+g+K_1,\tau)}{\omega_0^2(k+g)-(\omega_0(k+g+K_1)-\Omega)^2} \Big\} e^{i(\omega_0(k+g+K_1)-\Omega)\tau_0} \\
&- \frac{1}{\omega_0^2(k+g-K_2)-(\omega_0(k+g+2K_1-K_2)-2\Omega)^2} \frac{h_1(k+g+K_1-K_2) h_1(k+g+2K_1-K_2) a_0(k+g+2K_1-K_2,\tau)}{\omega_0^2(k+g+K_1-K_2)-(\omega_0(k+g+2K_1-K_2)-\Omega)^2} \\
&\times e^{i(\omega_0(k+g+2K_1-K_2)-\Omega)\tau_0} \\
&- \frac{1}{\omega_0^2(k+g-K_2)-(\omega_0(k+g+K_2)-2\Omega)^2} \frac{\alpha h_2(k+g)\alpha h(k+g+K_2) a_0(k+g+K_2,\tau)}{\omega_0^2(k+g)-(\omega_0(k+g+K_2)-\Omega)^2} e^{i(\omega_0(k+g+K_2)-\Omega)\tau_0} \Big\}
\end{aligned}
$$

The term B_3 gives

$$
\begin{aligned}
& ih_1(k+g+K_1)\Bigg\{\frac{1}{\omega_0^2(k+g+K_1)-(\omega_0(k+g-K_2)+2\Omega)^2}\Bigg\{-\frac{f_1(k+g)\alpha f_2(k+g-K_2)a_0(k+g-K_2,\tau)}{\omega_0^2(k+g)-(\omega_0(k+g-K_2)+\Omega)^2} \\
& -\frac{\alpha f_2(k+g+K_1-K_2)f_1(k+g-K_2)a_0(k+g-K_2,\tau)}{\omega_0^2(k+g+K_1-K_2)-(\omega_0(k+g-K_2)+\Omega)^2}\Bigg\}e^{i(\omega_0(k+g-K_2)+\Omega)\tau_0} \\
& -\frac{1}{\omega_0^2(k+g+K_1)-(\omega_0(k+g-K_1)+2\Omega)^2}\frac{f_1(k+g)f_1(k+g-K_1)a_0(k+g-K_1,\tau)}{\omega_0^2(k+g)-(\omega_0(k+g-K_1)+\Omega)^2}e^{i(\omega_0(k+g-K_1)+\Omega)\tau_0} \\
& -\frac{1}{\omega_0^2(k+g+K_1)-(\omega_0(k+g+K_1-2K_2)+2\Omega)^2} \\
& \times\frac{\alpha f_2(k+g+K_1-K_2)\alpha f_2(k+g+K_1-2K_2)a_0(k+g+K_1-2K_2,\tau)}{\omega_0^2(k+g+K_1-K_2)-(\omega_0(k+g+K_1-2K_2)+\Omega)^2}e^{i(\omega_0(k+g+K_1-2K_2)+\Omega)\tau_0}\Bigg\}
\end{aligned}
$$

Finally, B_4 gives

$$
\begin{aligned}
& i\alpha h_2(k+g+K_2)\Bigg\{\frac{1}{\omega_0^2(k+g+K_2)-(\omega_0(k+g-K_1)+2\Omega)^2}\Bigg\{-\frac{f_1(k+g-K_1+K_2)\alpha f_2(k+g-K_1)a_0(k+g-K_1,\tau)}{\omega_0^2(k+g-K_1+K_2)-(\omega_0(k+g-K_1)+\Omega)^2} \\
& -\frac{\alpha f_2(k+g)f_1(k+g-K_1)a_0(k+g-K_1,\tau)}{\omega_0^2(k+g)-(\omega_0(k+g-K_1)+\Omega)^2}\Bigg\}e^{i(\omega_0(k+g-K_1)+\Omega)\tau_0} \\
& -\frac{1}{\omega_0^2(k+g+K_2)-(\omega_0(k+g-2K_1+K_2)+2\Omega)^2}\frac{f_1(k+g-K_1+K_2)f_1(k+g-2K_1+K_2)a_0(k+g-2K_1+K_2,\tau)}{\omega_0^2(k+g-K_1+K_2)-(\omega_0(k+g-2K_1+K_2)+\Omega)^2} \\
& \times e^{i(\omega_0(k+g-2K_1+K_2)+\Omega)\tau_0} \\
& -\frac{1}{\omega_0^2(k+g+K_2)-(\omega_0(k+g-K_2)+2\Omega)^2}\frac{\alpha f_2(k+g)\alpha f_2(k+g-K_2)a_0(k+g-K_2,\tau)}{\omega_0^2(k+g)-(\omega_0(k+g-K_2)+\Omega)^2}e^{i(\omega_0(k+g-K_2)+\Omega)\tau_0}\Bigg\}
\end{aligned}
$$

We are not solving for the complete third-order solution but we gain insight into some of the terms. For instance consider a driving term of the form $\zeta e^{i(\omega_0(k+g+K_2)-\Omega)\tau_0}$ with $\zeta=\frac{1}{\omega_0^2(k+g-K_1)-(\omega_0(k+g+K_2)-2\Omega)^2}\xi$, then its contribution to the particular solution is $u_{3,P}^*=\frac{1}{\omega_0^2(k+g)-(\omega_0(k+g+K_2)-\Omega)^2}\zeta e^{i(\omega_0(k+g+K_2)-\Omega)\tau_0}$. Now these solutions will drive the fourth-order equation:

$$
\begin{aligned}
& \frac{\partial^2 u_4(k+g,\tau)}{\partial\tau_0^2}+2\frac{\partial^2 u_2(k+g,\tau)}{\partial\tau_0\partial\tau_2}+2\frac{\partial^2 u_0(k+g,\tau)}{\partial\tau_4\partial\tau_0}+\frac{\partial^2 u_0(k+g,\tau)}{\partial\tau_2^2}+v_a^2(k+g)^2u_4(k+g,\tau) \\
& =\{if_1(k+g-K_1)u_3(k+g-K_1,\tau)e^{+i\Omega\tau_0}+\alpha f_2(k+g-K_2)u_3(k+g-K_2,\tau)e^{i\Omega\tau_0} \\
& \quad +h_1(k+g+K_1)u_3(k+g+K_1,\tau)e^{-i\Omega\tau_0}+\alpha h_2(k+g+K_2)u_3(k+g+K_2,\tau)e^{-i\Omega\tau_0}\} \qquad \text{(A13)}
\end{aligned}
$$

The driving term $i\alpha f_2(k+g-K_2)u_3(k+g-K_2,\tau)e^{i\Omega\tau_0}$ will lead to secular terms of the form $i\alpha f_2(k+g-K_2)\frac{1}{\omega_0^2(k+g-K_2)-(\omega_0(k+g)-\Omega)^2}\frac{1}{\omega_0^2(k+g-K_1-K_2)-(\omega_0(k+g)-2\Omega)^2}\xi(k+g-K_2)e^{i\omega_0(k+g)\tau_0}$. In this expression $\xi(k+g-K_2)=if_1(k+g-K_1-K_2)\{-\frac{h_1(k+g-K_2)\alpha h_2(k+g)a_0(k+g,\tau)}{\omega_0^2(k+g-K_2)-(\omega_0(k+g)-\Omega)^2}-\frac{\alpha h_2(k+g-K_1)h_1(k+g)a_0(k+g,\tau)}{\omega_0^2(k+g-K_1)-(\omega_0(k+g)-\Omega)^2}\}$. This secular term will need to cancel in part the secular terms arising from $2\frac{\partial^2 u_0(k+g,\tau)}{\partial\tau_4\partial\tau_0}+\frac{\partial^2 u_0(k+g,\tau)}{\partial\tau_2^2}$ in Eq. (A13). Note that for doing this, we will need to use $a_0(k+g,\tau_4)=\alpha_0(\tau_4)e^{i\varphi(k+g)\tau_2}=\alpha_0^{'}e^{i\psi\tau_4}e^{i\varphi\tau_2}$ with the unknown quantity being ψ. Here we note that the quantity ξ is proportional to the quantity α. The secular terms proportional to α represent mixing of the two sinusoidal modulations. Indeed if $\alpha=0$, the problem reduces to that of a single sinusoidal modulation. The terms that contribute to the frequency correction of the zeroth-order bands are given in the main text [Eqs. (8a)–(8f)].

[1] A. A. Maznev, A. G. Every, and O. B. Wright, Reciprocity in reflection and transmission: What is a phonon diode, Wave Motion **50**, 776 (2013).

[2] P. A. Deymier, K. Runge, N. Swinteck, and K. Muralidharan, Torsional topology and fermion-like behavior of elastic waves in phononic structures, C. R. Acad. Sci. Mécan. **343**, 700 (2015).

[3] R. K. Pal, M. Schaeffer, and M. Ruzzene, Helical edge states and topological phase transitions in phononic systems using bi-layered lattices, J. Appl. Phys. **119**, 084305 (2016).

[4] R. Süsstrunk and S. D. Huber, Observation of phononic helical edge states in a mechanical topological insulator, Science **349**, 47 (2015).

[5] M. Xiao, G. Ma, Z. Yang, P. Sheng, Z. Q. Zhang, and C. T. Chan, Geometric phase and band inversion in periodic acoustic systems, Nat. Phys. **11**, 240 (2015).

[6] R. Fleury, D. L. Sounas, C. F. Sieck, M. R. Haberman, and A. Alu, Sound isolation and giant linear nonreciprocity in a compact acoustic circulator, Science **343**, 516 (2014).

[7] Q. Wang, Y. Yang, X. Ni, Y.-L. Xu, X.-C. Sun, Z.-G. Chen, L. Feng, X.-P. Liu, M.-H. Lu, and Y.-F. Chen, Acoustic asymmetric transmission based on time-dependent dynamical scattering, Sci. Rep. **5**, 10880 (2015).

[8] P. Wang, L. Lu, and K. Bertoldi, Topological Phononic Crystals with One-Way Elastic Edge Waves, Phys. Rev. Lett. **115**, 104302 (2015).

[9] N. Swinteck, S. Matsuo, K. Runge, J. O. Vasseur, P. Lucas, and P. A. Deymier, Bulk elastic waves with unidirectional backscattering-immune topological states in a time-dependent superlattice, J. Appl. Phys. **118**, 063103 (2015).

[10] C. Croenne, J. O. Vasseur, O. Bou Matar, M.-F. Ponge, P. A. Deymier, A.-C. Hladky-Hennion, and B. Dubus, Brillouin scattering-like effect and non-reciprocal propagation of elastic waves due to spatio-temporal modulation of electrical boundary conditions in piezoelectric media, Appl. Phys. Lett. **110**, 061901 (2017).

[11] M. B. Zanjani, A. R. Davoyan, A. M. Mahmoud, N. Engheta, and J. R. Lukes, One-way phonon isolation in acoustic waveguides, Appl. Phys. Lett. **104**, 081905 (2014).

[12] G. Trainiti and M. Ruzzene, Non-reciprocal elastic wave propagation in spatiotemporal periodic Structures, New J. Phys. **18**, 083047 (2016).

[13] H. Nassar, X. C. Xu, A. N. Norris, and G. L. Huang, Modulated phononic crystals: Non-reciprocal wave propagation and Willis materials, J. Mech. Phys. Solids **101**, 10 (2017).

[14] M. S. Kang, A. Butsch, and P. St. J. Russell, Reconfigurable light-driven opto-acoustic isolators in photonic crystal fibre, Nat. Photon. **5**, 549 (2011).

[15] Z. Yu and S. Fan, Complete optical isolation created by indirect interband photonic transitions, Nat. Photon. **3**, 91 (2009).

[16] D. W. Wang, H. T. Zhou, M. J. Guo, J. X. Zhang, J. Evers, and S. Y. Zhu, Optical Diode Made from a Moving Photonic Crystal, Phys. Rev. Lett. **110**, 093901 (2013)

[17] M. C. Rechtsman, J. M. Zeuner, Y. Plotnik, Y. Lumer, D. Podolsky, F. Dreisow, S. Nolte, M. Segev, and A. Szameit, Photonic Floquet topological insulators, Nature (London) **496**, 196 (2013).

[18] K. Fang, Z. Yu, and S. Fan, Realizing effective magnetic field for photons by controlling the phase of dynamic modulation, Nat. Photon. **6**, 782 (2012).

[19] A. Figotin and I. Vitebsky, Nonreciprocal magnetic photonic crystals, Phys. Rev. E **63**, 066609 (2001).

[20] J. A. Thomas, J. E. Turney, R. M. Iutzi, C. H. Amon, and A. J. H. McGaughey, Predicting phonon dispersion relations and lifetimes from the spectral energy density, Phys. Rev. B **81**, 081411 (2010).

[21] J. Gump, I. Finckler, H. Xia, R. Sooryakumar, W. J. Bresser, and P. Boolchand, Light-Induced Giant Softening of Network Glasses Observed near the Mean-Field Rigidity Transition, Phys. Rev. Lett. **92**, 245501 (2004).

[22] I. C. Khoo and Y. K. Wang, Multiple time scale analysis of an anharmonic crystal, J. Math. Phys. **17**, 222 (1976).